Infrared Physics & Technology 53 (2010) 457–463

Contents lists available at ScienceDirect

Infrared Physics & Technology

journal homepage: www.elsevier.com/locate/infrared

A new method for characterization of thermal properties of human enamel and dentine: Influence of microstructure

M. Lin [a], Q.D. Liu [a], T. Kim [b], F. Xu [a,c,*], B.F. Bai [d], T.J. Lu [a,*]

[a] Biomedical Engineering and Biomechanics Center, School of Aerospace, Xi'an Jiaotong University, Xi'an 710049, PR China
[b] School of Mechanical, Industrial and Aeronautical Engineering, University of the Witwatersrand, Private Bag 3, Johannesburg, South Africa
[c] HST-Center for Biomedical Engineering, Department of Medicine, Brigham and Women's Hospital, Harvard Medical School, Boston, MA, USA
[d] State Key Laboratory of Multiphase Flow in Power Engineering, Xi'an Jiaotong University, Xi'an 710049, PR China

ARTICLE INFO

Article history:
Received 18 July 2010
Available online 21 September 2010

Keywords:
Enamel
Dentine
Thermal diffusivity
Thermal conductivity
Microtubule
Infrared thermography

ABSTRACT

For better selection of "tooth-like" dental restorative materials, it is of great importance to evaluate the thermal properties of the human tooth. A simple method capable of non-destructively characterizing the thermal properties of the individual layers (dentine and enamel) of human tooth is presented. The traditional method of monotonic heating regime was combined with infrared thermography to measure the thermal diffusivities of enamel and dentine layers without physically separating them, with 4.08 ($\pm$0.178) $\times$ 10^7 m^2/s measured for enamel and 2.01 ($\pm$0.050) $\times$ 10^7 m^2/s for dentine. Correspondingly, the thermal conductivity was calculated to be 0.81 W/mK (enamel) and 0.48 W/mK (dentine). To examine the dependence of thermal conductivity on the configuration of dentine microstructure (microtubules), the Maxwell-Eucken and Parallel models of effective thermal conductivity are employed. The effective thermal conductivity of dentine in the direction parallel to tubules was found to be about 1.1 times higher than that perpendicular to the tubules, indicating weak anisotropy. By adopting the Series model, the bulk thermal conductivity of enamel and dentine layers is estimated to be 0.57 W/mK.

1. Introduction

With advances in modern dentistry, instruments of high energy intensities such as high power laser-based hand tools [1–3], light polymerizing units [4,5], and high-speed hand-pieces [6] have become a popular choice for dental treatments. Localized heat generation and its propagation through tooth tissues during the treatments cause localized temperature rises as well as non-uniform temperature distributions throughout tooth layers (enamel as the outer layer and dentine as the inner layer; see Fig. 1). The thermophysical properties of a tooth vary from one layer to another, and are anisotropic and inhomogeneous even in the individual layer [7,8]. The difference (mismatch) in thermal expansion coefficient between the enamel and dentine layers may induce thermal stresses and subsequent crack initiation and propagation through the enamel–dentine junction (EDJ) [9,10]. In addition, when the temperature within the pulp chamber (Fig. 1) exceeds a critical value (e.g., ∼42.5 °C), irreversible pulpal damage occurs [11,12]. Zach and Cohen [13] found experimentally that the healthy pulps of monkey tooth failed to recover in ∼60% of the cases if the intrapulpal temperature increases to 46.5 °C and ∼15% failed to recover when heated to 42.5 °C, with pulp necrosis (total irreversible damage) observed when the temperature reaches 52 °C.

Understanding the thermal behavior of human tooth is beneficial for optimizing clinical practice protocols and suggestions of daily substance intake [14]. This has, however, been hindered by the lack of detailed knowledge concerning tooth thermal behaviors including reliable experimental data on key thermal properties such as conductivity k and diffusivity α. Although numerous experimental methods have been developed to characterize the thermal performance of tooth tissues (enamel and dentine) using, for instance, thermocouples [15–18] and flash laser [19,20], several limitations associated with these methods exist: (i) destructing of tooth biological structure [15–20] is required which affects significantly the transfer of heat in tooth during measurement [21]; (ii) operating of the flash laser method has been restricted due to the high optical reflectivity (13.3–49.4%) of enamel [22]. Together with the generic dependence of thermal properties on sex, age and race, these limitations have resulted in large variations of existing experimental data on human tooth layers as listed in Table 1.

* Corresponding authors. Address: Biomedical Engineering and Biomechanics Center, School of Aerospace, Xi'an Jiaotong University, Xi'an 710049, PR China (T.J. Lu). Fax: +86 29 82665600.

E-mail addresses: fxu2@rics.bwh.harvard.edu (F. Xu), tjlu@mail.xjtu.edu.cn (T.J. Lu).

1350-4495/$ - see front matter © 2010 Elsevier B.V. All rights reserved.
doi:10.1016/j.infrared.2010.09.004

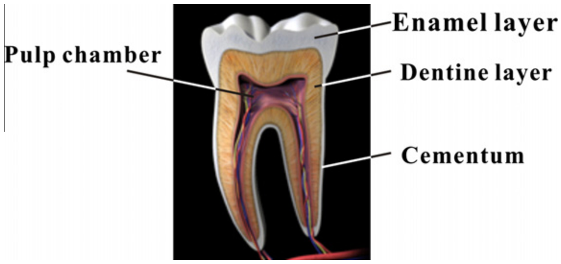

Fig. 1. A cut-away image of human tooth illustrating composite layers (www.3dscience.com).

Conventionally, the thermal diffusivity of tooth is calculated using tooth temperature measured as a function of time with, say, the monotonic heating regime (MHR) method [19]. However, in these studies, the enamel and dentine layers were typically treated as a bulk. Furthermore, an infinite Biot number ($Bi = \infty$) at the enamel border was assumed, corresponding to a step rise of tooth surface temperature (the first type thermal boundary condition). Such assumptions may cause significant errors as enamel and dentine have different thermal properties (due to difference in compositions and microstructures) and the Biot number is usually finite ($Bi < \infty$) in reality.

As a non-invasive temperature measurement method, the infrared (IR) thermography has been shown to be capable of measuring temperature field in small biological tissues [4]. In the present study, we intend to combine the traditional monotonic heating regime method with IR thermography, called here as the "modified monotonic heating regime (MMHR) method", to measure the thermal properties of human tooth for each layer (not as a bulk), without physically separating the enamel and dentine layers. With the advantage of whole temperature field measurement using the IR camera, the errors resulting from the effect of nonzero surface heat resistance can be corrected. The paper is organized as follows. Firstly, fundamental principles underlying the MMHR method and details of the experimental setup as well as tooth samples preparation are presented. The measured thermal diffusivities of enamel and dentine and as-calculated thermal conductivities are compared with those reported in the open literature. Secondly, to study the influence of dental tubules within the dentine layer on its thermal properties, the Maxwell-Eucken and Parallel models of effective thermal conductivity are employed. Finally, the thermal conductivity of tooth as a bulk (composite material) is estimated using the Series model based on obtained thermal conductivities of enamel and dentine layers.

2. Materials and method

2.1. Principles of modified monotonic heating regimes (MMHR) method

The thermal properties of a material dictate its response to temperature variations due to either heating or cooling. Amongst other thermal properties, the thermal diffusivity α has been correlated as a function of the characteristic time of thermal relaxation, which can be obtained in closed-form solution to the standard transient heat conduction equation for homogeneous materials [23]. The time-dependent heat conduction in a homogeneous-isotropic material can be described as [23]:

$$\frac{\partial T}{\partial t} = \alpha \nabla^2 T \tag{1}$$

With the assumptions of transient heat conduction in a semi-infinite plate (without internal heat source or heat sink) and temperature-independent physical properties, the solution to Eq. (1) subject to a step rise of constant temperature at the plate surface, $x = 0$, can be given in closed form by [23]:

$$\begin{aligned} T(x,t) &= T_\infty + C \sum_{n=1}^{\infty} A_n \cos\left(\mu_n \frac{x}{H}\right) \exp\left(-\frac{\mu_n^2 \alpha}{H^2} t\right) \\ &= f\left(\frac{x}{H}, Bi, F_0\right) \end{aligned} \tag{2}$$

Here, T_∞ is the plate temperature when reaching its steady-state, C is a constant independent of plate dimensions and thermal properties, H is the half-depth of the plate, h is the heat transfer coefficient on plate surface, k is the thermal conductivity of plate material (tooth tissue in this study), $Bi \equiv hH/k$ is the Biot number, $F_0 \equiv \alpha t/H^2$ is the Fourier number, and μ_n are the roots of the characteristic equation:

Table 1
Thermal properties of human tooth layers.

Property	Tooth component	Magnitude	References
α Thermal diffusivity ($\times 10^7$ m^2/s)	Enamel[a]	4.69	[15]
	Enamel	4.20	[16]
	Enamel[b]	2.27	[19]
	Dentine[a]	1.87[c], 1.83[d]	[15]
	Dentine[a]	1.99[c], 2.04~2.65[d]	[20]
	Dentine	2.58	[34]
	Dentine	2.60	[16]
	Dentine[b]	1.92	[19]
	Bulk value (enamel + dentine)	3.49 (heating), 2.78 (cooling)	[19]
k Thermal conductivity (W/mK)	Enamel[a]	0.93	[29]
	Enamel	0.92	[16]
	Dentine[a]	0.58[c], 0.57[d]	[29]
	Dentine	0.11	[35]
	Dentine	0.96	[17]
	Dentine	0.98	[36]
	Dentine	0.88	[31]
	Dentine[a]	0.36[c], 0.48~0.66[d]	[20]
	Dentine	0.63	[16]
	Dentine	0.40 (root)[d], 0.45 (crown)[d]	[37]

[a] From human third molar.
[b] From human premolar.
[c] Perpendicular to tubules.
[d] Parallel to tubules.

$$\cot(\mu) = \mu/Bi \tag{3}$$

It is known that a "regular regime" exists when $F_0 > 0.4$, within which the temperature change follows an exponential law [23,24] so that Eq. (2) can be reduced to:

$$T(x,t) = T_\infty + CA_1 \cos\left(\mu_1 \frac{x}{H}\right) \exp\left(-\frac{\mu_1^2 \alpha}{H^2} t\right) \tag{4}$$

Define the characteristic time of thermal relaxation τ_c as:

$$\tau_c = \frac{H^2}{\mu_1^2 \alpha} \tag{5}$$

Substitution of Eq. (5) into Eq. (4) leads to:

$$T(x,t) = T_\infty + CA_1 \cos\left(\mu_1 \frac{x}{H}\right) \exp\left(-\frac{t}{\tau_c}\right) \tag{6}$$

With the assumption of infinite Biot number ($Bi \to \infty$) at $x/H = 0$, Eq. (3) simplifies to:

$$\cos(\mu) = 0 \tag{7}$$

for which the first root is $\mu_1 = \pi/2$. This, together with Eq. (5), yields:

$$\alpha_\infty = \frac{4H^2}{\tau_c \pi^2} \tag{8}$$

As shown by MHR method that, in the case of transient heat transfer (assuming $Bi \to \infty$), τ_c is directly related to the thermal diffusivity (Eq. (8)) [23]. Once τ_c and H are experimentally determined, one can obtain the thermal diffusivity from Eq. (8). However, practically, Bi has finite values (the third type boundary condition), the experimental obtained τ_c may be expressed as [25]:

$$\tau_c = \tau_{conv} + \tau_{diff} \tag{9}$$

where τ_{diff} is the pure conduction contributed characteristic time and τ_{conv} is the pure convection contributed characteristic time (time delay due to the finite Biot number at $x/H = 0$). Eq. (8) can thence be re-expressed as [25]:

$$\alpha = \frac{4H^2}{\tau_c \pi^2} = \frac{4H^2}{(\tau_{diff} + \tau_{conv})\pi^2} \tag{10}$$

which, when $Bi = \infty$ and hence $\tau_{conv} = 0$, Eq. (10) reduces to:

$$\alpha = \frac{4H^2}{\tau_c \pi^2} = \frac{4H^2}{\tau_{diff} \pi^2} \tag{11}$$

Practically, Bi is finite and on the order of $\sim$2 in the case of hot water drinking (which imposes an average heat transfer coefficient of $h = 500$ W/mK at the tooth surface [26]). Therefore, Biot number for tooth during hot water heating is far form being assumed as infinite. When Bi is finite, so that $\tau_{conv} > 0$ (due to convection between hot/cold fluid and specimen surface), τ_c is contributed not only by τ_{diff} but also by τ_{conv} as indicated in Eq. (10). This will then induce a systematic deviation (error) if the classical monotonic heating regime method valid only for the case of $Bi \to \infty$ is adopted. Such deviation/error may be estimated as:

$$\text{Deviation} = \frac{\alpha_\infty - \alpha}{\alpha_\infty} = 1 - \frac{1}{1 + \tau_{conv}/\tau_{diff}} \tag{12}$$

For example, the systematic deviation is about 83.3% when τ_{conv}/τ_{diff} is 5.0. Correspondingly, $\tau_{conv}/\tau_{diff} \approx 50$ and the deviation exceeds 90% (the delay of temperature response due to boundary effect is inclusive in τ_{conv} here).

We assume that the thermal resistance acts in series: firstly, the resistance to convective transfer which is in proportional to τ_{conv} in the heated boundary; then, the resistance to diffusion through enamel which is inversely proportional to enamel thermal diffusivity; finally, the resistance through dentine which is inversely proportional to dentine thermal diffusivity. Thence, $\tau_{diff,e}$ in enamel layer and $\tau_{diff,d}$ in dentine layer could be separately written as:

$$\tau_{diff,e} = \tau_{DEJ} - \tau_{conv} \tag{13}$$

$$\tau_{diff,d} = \tau_{DPJ} - \tau_{DEJ} \tag{14}$$

where τ_{conv}, τ_{DEJ} and τ_{DPJ} are the characteristic time of temperature relaxation at enamel border (EB), enamel–dentine junction (EDJ) and dentine–pulp junction (DPJ). Hence, a MMHR method is proposed in the present study by modifying Eq. (8) as:

$$\alpha = \frac{4H^2}{(\tau_c - \tau_{conv})\pi^2} = \frac{4H^2}{\tau_{diff}\pi^2} \tag{15}$$

Corrected $\tau_{diff,e}$ and $\tau_{diff,d}$ may therefore be determined if τ_{conv}, τ_{DEJ} and τ_{DPJ} are estimated from experimental measurements (MMHR method). Then, α can be determined using Eq. (15) (note that the determination of α in this study does not involve determination of the Biot number). By taking the advantage of multi-point temperature measurement with an IR camera, this challenge is addressed below.

2.2. Sample preparation

Intact human molar tooth extracted from a unknown adult patient for orthodontic purposes was stored in saline solution at 4 °C [27]. The tooth was then sliced longitudinally into two halves using a diamond-bladed saw (Buchler Ltd. ISOMET 1000). For temperature measurements, one of the sliced surfaces was polished and painted in black to enhance its emissivity for the IR camera. Subsequently, the specimen was mounted in a thin resin plate, as shown schematically in Fig. 2a. The thickness of the tooth sample and that of the resin plate was approximately 3 mm and 0.5 mm, respectively. To avoid water leakage during measurement, four screw bolts were used to tighten the specimen (Fig. 2a). Fig. 2b shows the side view of the test setup, with the direction of water flow indicted by an arrow. For thermal insulation, a layer of gypsum (thermal conductivity $\sim$0.09 W/mK) was used to surround the specimen as shown in Fig. 2b, such that only the occlusal surface of the sliced tooth was exposed to thermal loading.

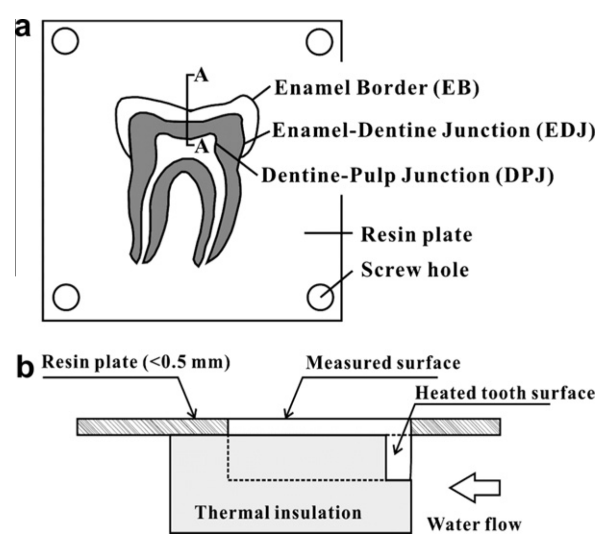

Fig. 2. Schematic of experimental setup: (a) tooth sample mounted in a thin resin plate, showing enamel border (EB), enamel-dentine junction (EDJ) and dentine-pulp junction (DPJ); (b) cross-sectional view of as prepared sample and its heating pattern.

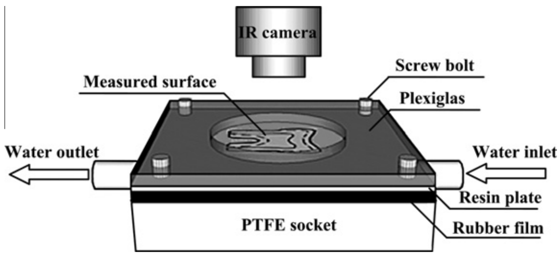

Fig. 3. Test rig for surface temperature measurement with IR camera.

2.3. Experimental procedures

The test rig is depicted schematically in Fig. 3. The thermostatic system for distilled water circulation which imposes a step (or steep) rise of water temperature at the occlusal surface of tooth (Fig. 2b) was equipped with a thermostat and pump. Prior to the experiment, it was established that the temperature of the circulating water was stable, with less than ±0.1 °C fluctuation with respect to a set temperature. A Polytetrafluoroethylene (PTFE) stand machined with a circular socket (40 mm in diameter) was connected to the thermostat tank. The tooth specimen mounted in resin was placed on the socket of the PTFE stand and fixed with screw bolts. A thin rubber film having a 40 mm diameter hole at its center was inserted between the resin plate and the PTFE stand to prevent water leakage. Before heating the distilled water, the circular socket was first circulated with distilled water at room temperature (∼24.5 °C) to exclude air bubbles. The circulation was then turned off and the distilled water in the tank was heated up to a set temperature (e.g., 60 °C) regulated by the thermostat. The tooth sample was then exposed to convective flow of hot water for 500 s. An infrared camera (NEC, TH9100 MV) was positioned normal to the tooth sample to monitor the evolution of its surface temperature (Fig. 3). The camera, pre-calibrated as described in a previous study [21], is capable of measuring temperature ranging from −20 to 100 °C with a resolution of ±0.1 °C. The working wavelength of the camera ranges from 8 to 14 μm and has a sampling rate of 30 frames per second. To store automatically the captured images, the camera was connected to a personal computer.

3. Results and discussion

3.1. Thermal properties of enamel and dentine layers

Fig. 4a presents temperature contours on the surface of the sliced tooth sample captured by the IR camera at $t = 30$ s after heating is started. High temperature gradients are observed, which is attributed to the layer-like composite structure of tooth and the different thermal properties of enamel and dentine layers. To estimate the characteristic time τ_c, the temporal variation of temperature at selected locations, e.g., EB, EDJ and DPJ (along section A–A, see Fig. 2a), are plotted in Fig. 4b. As indicated by Eq. (15), the thickness (2H) of each tooth layer needs to be estimated to determine its thermal diffusivity. To this end, the thickness of each layer was measured along section A–A using an optical microscopy, with $H_{\mathrm{enamel}} = 2.4$ mm obtained for the enamel layer and $H_{\mathrm{dentine}} = 3.8$ mm for the dentine layer.

Following the method described in detail in Refs. [19,23,25,28], the characteristic time τ_c of each tooth layer was evaluated by fitting the temperature curve using the exponential function. Fig. 5 shows an example of temperature data fitting for the DPJ. After removing the initial part of the temperature rise, the remaining data corresponding to the "regular regime" (i.e., $F_0 > 0.4$) was fitted

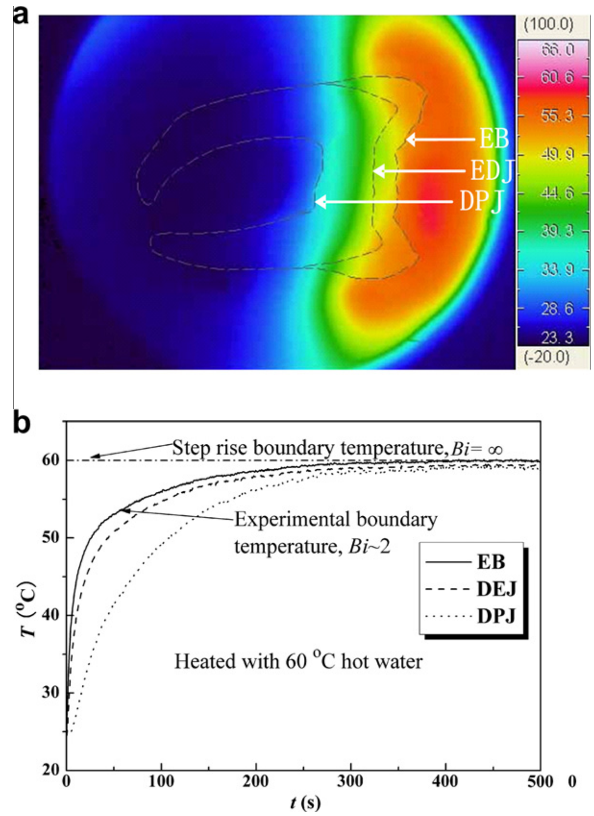

Fig. 4. Surface temperature field of sliced human tooth: (a) temperature contours at $t = 30$ s after heating; (b) temporal evolution of temperature at enamel border (EB), enamel–dentine junction (EDJ), and dentine–pulp junction (DPJ).

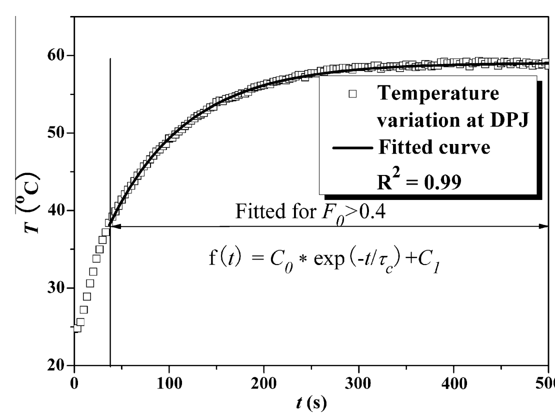

Fig. 5. Curve fitting of temperature evolution at DPJ illustrating how the characteristic time is estimated from transient temperature response at a selected location: $C_0 = -32.740$, $\tau_c = 81.77$ s, $C_1 = 59.057$.

with the exponential function, from which τ_c was estimated to be 81.77 s. Similarly, τ_c was estimated for the EDJ and EB, and the results are listed in Table 2. The diffusion characteristic time τ_{diff} of

Table 2
Characteristic time τ_c of temperature relaxation at enamel border (EB), enamel-dentine junction (EDJ) and dentine-pulp junction (DPJ); calculated conductive characteristic time for enamel ($\tau_{\mathrm{diff,}}$) and dentine ($\tau_{\mathrm{diff,\ d}}$).

Locations	EB	EDJ	DPJ
τ_c (s)	73.08[a]	74.51[a]	81.77[a]
$\tau_{\mathrm{diff,e}} = \tau_{\mathrm{DEJ}} - \tau_{\mathrm{conv}}$ (s)	–	1.43	–
$\tau_{\mathrm{diff,d}} = \tau_{\mathrm{DPJ}} - \tau_{\mathrm{DEJ}}$ (s)	–	–	7.26

[a] Averaged value.

Table 3
Thermal properties of human tooth (as a bulk composite), enamel and dentine calculated form experimental data, with density ρ and specific heat c_p taken from Refs. [15,20].

Specimens	Enamel	Dentine	Tooth composite
Thermal diffusivity α ($\times 10^7$ m^2/s)	4.08 (±0.178)	2.01 (±.050)	2.06 3.49 [19]
Specific heat c_p (J/kg K)	710 [15]	1066.4 [20]	1260 [15]
Density ρ (kg/m^3)	2800 [15]	2248 [20]	2200 [15]
Thermal conductivity k (W/m K)	0.81	0.48	0.57 0.97 [19]

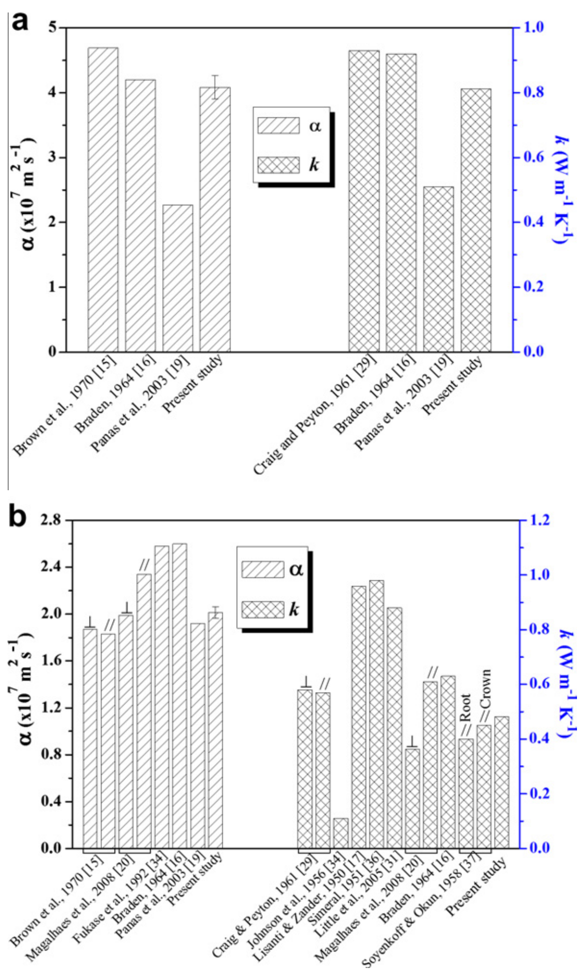

Fig. 6. Measured thermal diffusivity of human tooth compared with those reported in open literature: (a) enamel; (b) dentine. Heat flow direction relative to dentine tubules: parallel (//); perpendicular (⊥).

each tooth layer calculated using Eqs. (13) and (14) are listed in Table 2. For known $\tau_{\mathrm{diff,e}}$ and τ_{conv}, Bi could be determined as flowing. Combine Eqs. (5) and (9), then, put together with Eq. (15), yields:

$$\mu_1 = \frac{\pi}{2}\sqrt{\tau_{\mathrm{diff,e}}/(\tau_{\mathrm{conv}} + \tau_{\mathrm{diff,e}})} \tag{16}$$

Assuming μ_1 ($\mu_1 \approx 0.2$) is small, the second-order Taylor expansion of Eq. (3) generates:

$$Bi \approx \frac{2\mu^2}{2-\mu^2} \tag{17}$$

Substitute Eq. (16) to Eq. (17), one obtains an approximate analytical expression for Bi:

$$Bi \approx \frac{2\pi^2}{8-\pi^2+8(\tau_{\mathrm{conv}}/\tau_{\mathrm{diff,e}})} \tag{18}$$

In the present study Bi was estimated to be ~0.048 which is typically small Biot number as compared with that ~2 adopted form ancient Ref. [26].

The dashed dot curve in Fig. 4b shows a step rise of temperature at the EB, corresponding to the idealized case of infinite Biot number ($Bi = \infty$). The measured temperature at the EB as shown by the solid curve in Fig. 4b corresponds to a finite Biot number. Therefore, a modification of the infinite Bi case needs to be carried out to account for such deviation as described in Section 2.1. The thermal diffusivities of the enamel and dentine layers were calculated using Eq. (15), as summarized in Table 3. Correspondingly, the thermal conductivity k of each layer was calculated as:

$$k = \alpha\rho c_p \tag{19}$$

where ρ and c_p are the density and specific heat of the tooth layer (Table 3).

Fig. 6a compares the thermal diffusivity of enamel obtained from the present study with those reported in the open literature. Braden [16] found $\alpha = 4.20 \times 10^{-7}$ m^2/s for enamel using the thermocouple-based method, whilst Brown et al. [15] obtained $\alpha = 4.69 \times 10^{-7}$ m^2/s, both in good agreement with the present data $\alpha = 4.08 \times 10^{-7}$ m^2/s. On the other hand, using the flash laser method, Panas et al. [19] found that $\alpha = 2.27 \times 10^{-7}$ m^2/s, which is considerably lower. In addition to the influence of dental filling material (the cylindrical sample of diameter 12 mm was prepared by filling irregular enamel pieces with dental material [19]), enamel has a high optical reflectivity, accounting for about 13.3 ~ 49.4% (depending on the laser wave length) of energy loss when irradiated by laser beams [22]. This indicates that the flash laser method (despite of its high measurement accuracy) may not be suitable for measuring the thermal diffusivity of materials having a high optical reflectivity (e.g., enamel). Based on the present data of thermal diffusivity, the thermal conductivity of enamel was calculated to be $k = 0.81$ W/mK (Fig. 6a), which is consistent with the data reported by Craig and Peyton [29] and Braden [16]. The conductivity found by Panas et al. [19] for enamel is significantly lower due to the small value of α.

In a similar manner, the estimated thermal diffusivity and conductivity of the dentine layer are plotted in Fig. 6b and compared with the existing data. The present data $\alpha = 2.01 \times 10^{-7}$ m^2/s falls within the range between 2.34×10^{-7} m^2/s and 1.92×10^{-7} m^2/s obtained by Magalhães et al. [20] and Panas et al. [19] using the flash laser method. Compared with enamel, the reflectivity of dentine is relatively low, ranging from 8.6% to 16.7% [22]. Hence, the measurement of α with the flash laser method is reliable for dentine. It should be noticed that the thermal conductivity of human dentine was found to vary in the range of 0.36 and 0.88 W/mK [15,16,20,30,31]. The present estimate $k = 0.48$ W/mK falls within this range.

In summary, it is demonstrated that combining the monotonic heating regime method with the infrared thermography provides reasonable estimates of thermal diffusivity and conductivity for enamel and dentine layers without physically separating them. It should be mentioned that the reliability of the proposed method is mainly dependent on the special and temperature resolution of the IR camera when applying it on another specimen.

3.2. Influence of microstructure in direction-dependent dentine thermal property

It is seen from the data of Fig. 6b that the thermal conductivity of dentine shows weak anisotropic, which may be attributed to the presence of dentine tubules [15,20,29]; see Fig. 7a. As the thermal conductivity of these tubules is considerably smaller than that of the solid dentine material (*in vitro*), they act to reduce the bulk

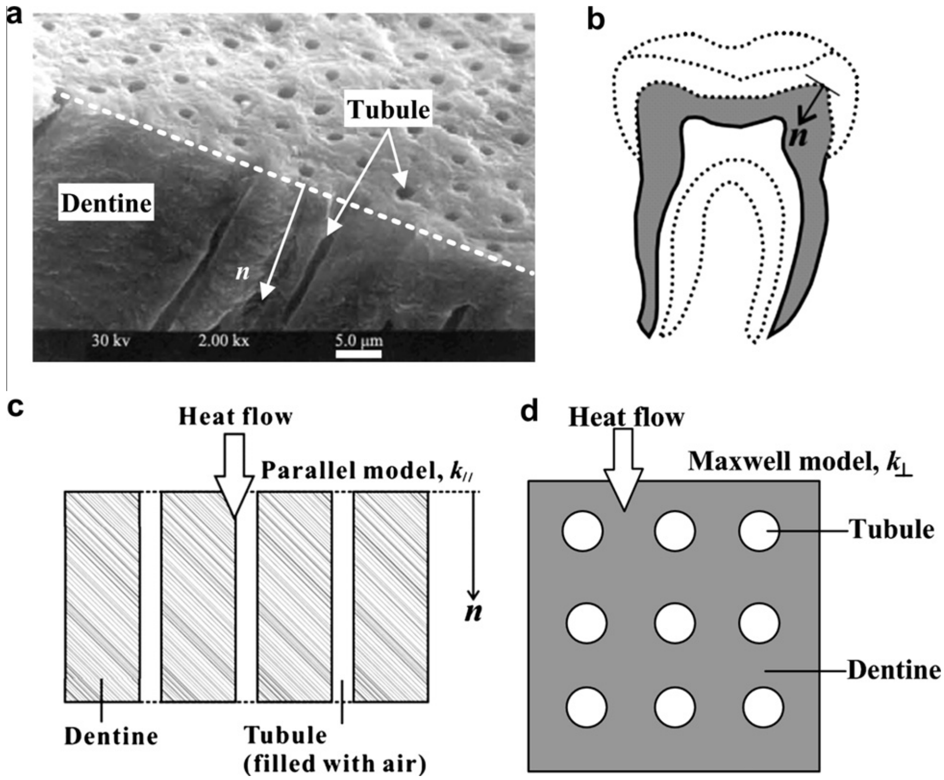

Fig. 7. (a) SEM image of human dentine showing solid dentine material and tubules [33]; (b) schematic of heat flow direction across tooth (normal to EDJ); (c) modeling of heat flow across dentine with Parallel model; (d) modeling of heat flow across dentine with Maxwell-Eucken model.

thermal conductivity of the dentine layer [20]. This section aims to investigate whether the configuration and volume fraction of the dentine tubules affect the direction-dependent thermal conductivity of dentine.

The effective thermal conductivity of a heterogeneous material such as human tooth is strongly affected by its composition and structure [32]. Correspondingly, numerous effective conductivity models have been developed. In view of the topological configuration of dentine tubules (Fig. 7a), the Maxwell-Eucken and Parallel models appear to be suitable since the cylindrical tubules in the present study are parallel to the direction of heat flow (i.e., perpendicular to the EDJ interface; see Fig. 7b).

Fig. 7a shows the SEM (scanning electron microscope) image of cylindrical microchannel-like tubules distributed in the body of dentine, which radiate through the dentine from the pulpal wall to the exterior cementum or the enamel–dentine junction [33]. Fig. 7c and d presents two-dimensional (2D) sketch of dentine microstructure and the effective thermal conductivity models employed. Let $k_{//}$ and $k_{\perp}$ denote the effective thermal conductivity of dentine in the direction parallel and perpendicular to the dentine tubules, respectively. Let k_d denote the thermal conductivity of solid dentine material and k_t represent the thermal conductivity of the medium filling the tubules (assumed to be air in this study, with $k_t = 0.023$ W/mK). Let V_d and V_t be the volume fraction of the solid dentine and tubules, respectively. In view of the orientation of dentine tubules relative to the direction of heat flow as shown in Fig. 7c and d, applying separately the Parallel and Maxwell-Eucken models [32] to the idealized configuration of Fig. 7c and d, we obtain:

$$k_{//} = V_d k_d + V_t k_t \tag{20}$$

$$k_{\perp} = k_d \frac{2k_d + k_t - 2(k_d - k_t)V_t}{2k_d + k_t + (k_d - k_t)V_t} \tag{21}$$

from which:

$$\frac{k_{//}}{k_{\perp}} = \frac{\left[(1 - V_t)\frac{k_d}{k_t} + V_t\right]\left[2\frac{k_d}{k_t} + 1 + (\frac{k_d}{k_t} - 1)V_t\right]}{\frac{k_d}{k_t}\left[2\frac{k_d}{k_t} + 1 - 2(\frac{k_d}{k_t} - 1)V_t\right]} \tag{22}$$

Typically, while the overall thermal conductivity (either $k_{//}$ or $k_{\perp}$) of dentine lie between 0.36 and 0.88 W/mK, the ratio k_d/k_t has a value of approximately 20 [16,20,29,31].

Based on Eq. (22), the influence of tubule volume fraction V_t on the effective thermal conductivity ratio $k_{//}/k_{\perp}$ is presented in Fig. 8. When V_t is increased from 0% to 20% [20,33], $k_{//}/k_{\perp}$ increases from 1.00 to 1.10. A weak dependence of $k_{//}/k_{\perp}$ on V_t is observed, though $k_{//}$, $k_{\perp}$ decrease separately with the increasing of V_t (as determined by Eqs. (20) and (21)). The value of the ratio (~1.00) also indicates

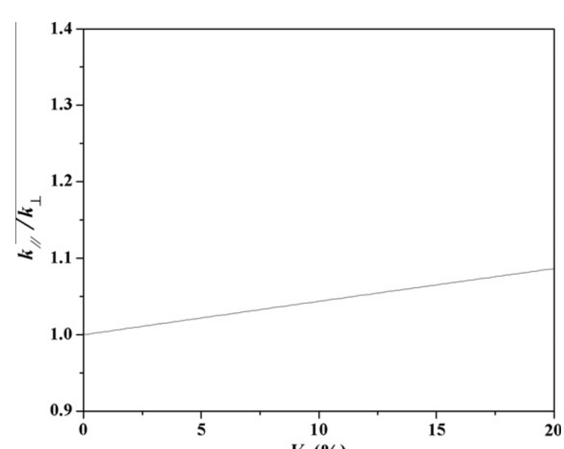

Fig. 8. Effective thermal conductivity ratio of dentine plotted as a function of dentine tubule volume fraction, with $k_d/k_t = 20$.

weak anisotropic thermal conductivity in dentine layer. This is in consistence with the experimental findings made by Magalhães et al. [20].

3.3. Apparent (bulk) tooth thermal properties

Applying Eq. (8), Panas et al. [19] estimated the apparent thermal diffusivity of human tooth. However, this is associated with two major limitations: (1) the assumption of infinite Biot number at the boundary, which leads to an overestimation of τ_c [23,25]; (2) Eq. (8) is not suitable for composite materials such as tooth [23].

Judging from the topology of human tooth, we can assume that the enamel and dentine layers are stacked in a series manner. By adopting the Series model, the apparent thermal conductivity k_{app} of the two layers may be estimated as:

$$1/k_{\mathrm{app}} = \left(\frac{H_{\mathrm{enamel}}/k_{\mathrm{enamel}} + H_{\mathrm{dentine}}/k_{\mathrm{dentine}}}{H_{\mathrm{enamel}} + H_{\mathrm{dentine}}}\right) \tag{23}$$

where (H_{enamel}, H_{dentine}) and (k_{enamel}, k_{dentine}) are the thickness and effective thermal conductivity of the enamel and dentine layers, respectively. Based on the present measurement data, the effective thermal conductivity of enamel and dentine layers are separately 0.81 and 0.48 W/mK as listed in Table 3. Using Eq. (23), we obtain k_{app} = 0.57 W/mK, which corresponds to an apparent thermal diffusivity of 2.06×10^{-7} m^2/s. Table 3 shows the presently estimated apparent thermal conductivity and diffusivity, both are significantly smaller than those predicted by Panas et al. [19].

4. Conclusions

By combining the monotonic heating regime method with the technique of IR thermography, a simple experimental method for estimating the thermal properties (conductivity and diffusivity) of human tooth is developed. The proposed method was validated by measuring human tooth thermal properties *in vitro*. Whilst the measurement was carried out without destructing the tooth biological junction, errors resulting from a nonzero surface heat resistance effect are corrected. The present results agree well with existing data obtained using traditional methods based on thermocouples and flash laser method. It is demonstrated that the presence of dentine tubules has a strong influence on the overall thermal conductivity of dentine ($k_{//}$ and $k_{\perp}$). Whereas, dentine tubules has a negligible influence on the ratio $k_{//}/k_{\perp}$ indicating a weak direction-dependence thermal conductivity in dentine layer.

Acknowledgements

This work is supported by the National Natural Science Foundation of China (10632060, 10825210, 81000453), the National 111 Project of China (B06024), and the National Basic Research Program of China (2006CB601202).

References

[1] M. Fahey, O. Onyejekwe, H. Lawrence Mason, K. Mitra, Precise dental ablation using ultrashortpulsed 1552 nm laser, Int. J. Heat. Mass. Trans. 51 (2008) 5732–5739.
[2] A.U. Eldeniz, A. Usumez, S. Usumez, N. Ozturk, Pulpal temperature rise during light-activated bleaching, Mater. Res. Part B 72B (2005) 254–259.
[3] B.S. Lee, C.W. Chang, W.P. Chen, W.H. Lan, C.P. Lin, In vitro study of dentin hypersensitivity treated by Nd : YAP laser and bioglass, Dent. Mater. 21 (2005) 511–519.
[4] A. Uhl, R.W. Mills, K.D. Jandt, Polymerization and light-induced heat of dental composites cured with LED and halogen technology, Biomaterials 24 (2003) 1809–1820.
[5] S. Bouillaguet, G. Caillot, J. Forchelet, M. Cattani-Lorente, J.C. Wataha, I. Krejci, Thermal risks from LED- and high-intensity QTH-curing units during polymerization of dental resins, J. Biomed. Mater. Res. Part B 72B (2005) 260–267.
[6] B.N. Cavalcanti, J.L. Lage-Marques, S.M. Rode, Pulpal temperature increases with Er:YAG laser and high-speed handpieces, J. Pros. Dent. 90 (2003) 447–451.
[7] A. Kishen, U. Ramamurty, A. Asundi, Experimental studies on the nature of property gradients in the human dentine, J. Biomed. Mater. Res. Part A 51 (2000) 650–659.
[8] A. Kishen, A. Asundi, Investigations of thermal property gradients in the human dentine, J. Biomed. Mater. Res. 55 (2001) 121–130.
[9] W.S. Brown, H.R. Jacobs, R.E. Thompson, Thermal fatigue in teeth, J. Dent. Res. 51 (1972) 461–467.
[10] H.R. Jacobs, R.E. Thompson, W.S. Brown, Heat transfer in teeth, J. Dent. Res. 52 (1973) 248–252.
[11] M. Sulieman, J.S. Rees, M. Addy, Surface and pulp chamber temperature rises during tooth bleaching using a diode laser: a study in vitro, Brit. Dent. J. 200 (2006) 631–634.
[12] M. Pohto, A. Scheinin, Microscopic observations on living dental pulp II. The effect of thermal irritants on the circulation of the pulp in the lower rat incisor, Acta Odontol. Scand. 16 (1958) 315–327.
[13] L. Zach, G. Cohen, Pulp response to externally applied heat, Oral Surg. Oral Med. Oral Pathol. Oral Radiol. Endodont. 19 (1965) 515–530.
[14] M. Lin, F. Xu, T.J. Lu, B.F. Bai, A review of heat transfer in human tooth—experimental characterization and mathematical modeling, Dent. Mater. 26 (2010) 501–513.
[15] W.S. Brown, W.A. Dewey, H.R. Jacobs, Thermal properties of teeth, J. Dent. Res. 49 (1970) 752–755.
[16] M. Braden, Heat conduction in teeth and the effect of lining materials, J. Dent. Res. 43 (1964) 315–322.
[17] V.F. Lisanti, H.A. Zander, Thermal conductivity of dentin, J. Dent. Res. 29 (1950) 493–497.
[18] R. Phillips, R.H. Reinking, L.J. Phillips, Thermal conductivity of dental cement-a method and determinations for three commercial materials, J. Dent. Res. 33 (1954) 511–518.
[19] A.J. Panas, S. Żmuda, J. Terpiłowski, M. Preiskorn, Investigation of the thermal diffusivity of human tooth hard tissue, Int. J. Thermophys. 24 (2003) 837–848.
[20] M.F. Magalhães, R.A.N. Ferreira, P.A. Grossi, R.M. Andrade, Measurement of thermophysical properties of human dentin: effect of open porosity, J. Dent. 36 (2008) 588–594.
[21] M. Lin, Q.D. Liu, F. Xu, B.F. Bai, T.J. Lu, In vitro investigation of heat transfer in human tooth, in: The International Conference on Experimental Mechanics, SPIE: Singapore, 2009.
[22] D. Fried, R.E. Glena, J.D.B. Featherstone, W. Seka, Permanent and transient changes in the reflectance of CO_2 laser-irradiated dental hard tissues at lambda = 9.3, 9.6, 10.3, and 10.6 mu m and at fluences of 1–20 J/cm^2, Lasers Surg. Med. 20 (1997) 22–31.
[23] K.D. Maglić, A. Cezairliyan, V.E. Peletsky, Compendium of Thermophysical Property Measurement Methods V1 Survey of Measurement Techniques, Plenum Press, New York, 1984. pp. 430–453.
[24] H.S. Carlslaw, J.C. Jaeger, Conduction of Heat in Solids, Oxford University Press, London, 1959. pp. 100–240.
[25] A.J. Panas, J. Sypek, Validation of the thermal diffusivity from modified monotonic heating regime procedure, Int. J. Thermophys. 27 (2006) 1844–1858.
[26] J.H. de Vree, T.A. Spierings, A.J. Plasschaert, A simulation model for transient thermal analysis of restored teeth, J. Dent. Res. 62 (1983) 756–759.
[27] P. Linsuwanont, J.E.A. Palamara, H.H. Messer, An investigation of thermal stimulation in intact teeth, Arch. Oral Biol. 52 (2007) 218–227.
[28] A.J. Panas, M. Preiskorn, M. Dabrowski, S. Zmuda, Validation of hard tooth tissue thermal diffusivity measurements applying an infrared camera, Infrared Phys. Tech. 49 (2007) 302–305.
[29] R.G. Craig, F.A. Peyton, Thermal conductivity of tooth structure, dental cements and amalgam, J. Dent. Res. 40 (1961) 411–417.
[30] B.C. Soyenkoff, O. JH, Thermal conductivity measurements of dental tissues with the aid of thermistors, J. Am. Dent. Assoc. 57 (1958) 23–30.
[31] P.A.G. Little, D.J. Wood, N.L. Bubb, S.A. Maskill, L.H. Mair, C.C. Youngson, Thermal conductivity through various restorative lining materials, J. Dent. 33 (2005) 585–591.
[32] J.K. Carson, S.J. Lovatt, D.J. Tanner, A.C. Cleland, Thermal conductivity bounds for isotropic, porous materials, Int. J. Heat. Mass. Trans. 48 (2005) 2150–2158.
[33] D.H. Pashley, Dynamics of the pulpo-dentin complex, Crit. Rev. Oral Biol. Med. 7 (1996) 104–133.
[34] Y. Fukase, M. Saitoh, M. Kaketani, M.N.M. Ohashi, Thermal coefficients of paste–paste type pulp capping cements, Dent. Mater. J. 11 (1992) 189–196.
[35] R.J. Johnson, L.J. Phillips, R.W. Phillips, An improved method for measuring the coefficient of thermal conductivity of dental cement, Am. Dent. Assoc. 53 (1956) 577–583.
[36] W.G. Simeral, Thermal Conductivity of Dental Materials, Microfilm of Papers Presented at the Annual IADR. Dental Materials Group Meeting, March, 1951. J. Dent. Res. 30 (1951) 499 (abstract).
[37] B.C. Soyenkoff, J.H. Okun, Thermal conductivity measurements of dental tissues with the aid of thermistors, J. Am. Dent. Assoc. 57 (1958) 23–30.